J Therm Anal Calorim (2010) 99:349–356
DOI 10.1007/s10973-009-0272-4

Synthesis and thermal decomposition kinetics of two lanthanide complexes with cinnamic acid and 2,2′-Bipyridine

L. Tian · N. Ren · J. J. Zhang · H. M. Liu · S. J. Sun · H. M. Ye · K. Z. Wu

Received: 2 March 2009 / Accepted: 23 June 2009 / Published online: 6 August 2009

Abstract The two complexes of $[Ln(CA)_3bipy]_2$ (Ln = Tb and Dy; CA = cinnamate; bipy = 2,2′-bipyridine) were prepared and characterized by elemental analysis, infrared spectra, ultraviolet spectra, thermogravimetry and differential thermogravimetry techniques. The thermal decomposition behaviors of the two complexes under a static air atmosphere can be discussed by thermogravimetry and differential thermogravimetry and infrared spectra techniques. The non-isothermal kinetics was investigated by using a double equal-double steps method, the nonlinear integral isoconversional method and the Starink method. The mechanism functions of the first decomposition step of the two complexes were determined. The thermodynamic parameters ($\Delta H^{\neq}$, $\Delta G^{\neq}$ and $\Delta S^{\neq}$) and kinetic parameters (activation energy E and the pre-exponential factor A) of the two complexes were also calculated.

Keywords Thermal decomposition mechanism · Non-isothermal kinetics · Lanthanide complexes

L. Tian · J. J. Zhang (✉) · S. J. Sun · H. M. Ye
Experimental Center, Hebei Normal University,
Shijiazhuang 050016, People's Republic of China
e-mail: jjzhang6@126.com

L. Tian · S. J. Sun · H. M. Ye · K. Z. Wu
College of Chemistry and Material Science, Hebei Normal University, Shijiazhuang 050016, People's Republic of China

N. Ren
Department of Chemistry, Handan College,
Handan 056005, People's Republic of China

H. M. Liu
College of Chemistry and Pharmacy Engineering,
Hebei University of Science and Technology,
Shijiazhuang 050018, People's Republic of China

Introduction

Rare-earth ions and organic carboxylic acids can form stable rare earth carboxylic acid complexes. Much work has been gained in research of them in many fields, such as extraction and separation of rare earth elements, bactericidal, polymerization catalytic of polymer [1–5], etc. This kinds of complexes as efficient luminescent materials have many applications, such as new rare-earth fluorescent materials, luminescent probes in biomedical assays, emitters in electroluminescent (EL) devices, etc. In addition, these complexes have drawn great attention among scholars because of their structures and thermal stability [5–10]. Therefore, the kinds of complexes as a part of materials chemistry have important theoretical significance and research value. The thermal stability investigation enables to reveal the important information about the properties of these complexes and enriches the research contents of rare-earth complexes. The reason that these complexes have unique properties due to the special structures, and the studying for the thermal properties of complexes can also help to understand the structures themselves.

In previous studies [11–15], a series of ternary rare-earth complexes with benzoic acid or its derivatives and nitrogen-containing ligands were prepared, and their crystal structures, thermal decomposition behaviors and non-isothermal kinetics were also reported. We select cinnamic acid as ligand in this paper. During the period of biosynthesis, cinnamic acid is the precursor substances of salicylic acid which is the endogenous signal molecule in plant [16]. Solid state compounds of cinnamic acid with a series of lanthanide (III) including La, Ce, Pr, Nd and Sm have been previously prepared and studied by TG, DTG and DSC [17]. Then the synthesis, spectra, anti-inflammatory action and XPS of ternary lanthanide (Ce, Nd and Eu) complexes of cinnamic acid and phenanthroline have also been reported [16, 18]. Therefore, here we report the synthesis and the thermal decomposition kinetics of $[Ln(CA)_3bipy]_2$ (Ln = Tb and Dy; CA = cinnamate; bipy = 2,2′-bipyridine). Meanwhile, the non-isothermal kinetics was discussed by using a double equal-double steps method [19], the nonlinear integral isoconversional method (NL-INT) [20] and the Starink method [21].

Experimental

Materials

All the reagents used were A. R. grade and used without further purification.

Synthesis of the title complexes

A stoichiometric amount of $LnCl_3 \cdot 6H_2O$ (Ln = Tb and Dy), cinnamic acid and 2,2′-bipyridine were dissolved into 95% ethanol, respectively. The pH value of cinnamic acid solution was adjusted to 6–7 with NaOH (1 mol L^{-1}). The ethanol solution of the two ligands was mixed and then added dropwise to the $LnCl_3 \cdot 6H_2O$ solution. And then the mixture was stirred for 8 h at room temperature and deposited for 12 h. Subsequently, the precipitates were collected by filtration and then dried in air.

Apparatus and conditions of experiment

The contents of carbon, hydrogen and nitrogen were acquired on a Vario-EL III element analyzer, while the metal content was assayed using EDTA titration method. Infrared spectra were recorded at room temperature from 4,000 to 400 cm^{-1} using a Perkin-Elmer FTIR-1730 spectrometer with KBr discs. The ultraviolet spectra were recorded on a Shimadzu 2501 spectrophotometer in DMSO. The TG-DTG experiments of the title complexes were achieved using a Perkin-Elmer TGA7 thermogravimetric analyzer. The heating rate was 3, 5, 7, 10, 15 K min^{-1} from ambient to 1,223.15 K under a static air atmosphere.

Methodology and kinetic analysis

The double equal-double steps method [19], the nonlinear integral isoconversional method [20] and the Starink method [21] were used to study the thermal decomposition kinetics of the two title complexes, whose basic principles are as follows:

Double equal-double steps method

Determination of the function of conversion

The equations of iterative calculation in an accurate kinetic studying [22] are as follows:

$$\ln\frac{\beta}{H(x)} = \left\{\ln\left[\frac{0.0048AE}{R}\right] - \ln G(\alpha)\right\} - 1.0516\frac{E}{RT} \qquad (1)$$

Thereinto:

$$H(x) = \frac{\exp(-x)}{0.0048\exp(-1.0516x)}h(x)$$

$$h(x) = \frac{x^4 + 18x^3 + 86x^2 + 96x}{x^4 + 20x^3 + 120x^2 + 240x + 120}$$

$$\begin{aligned}\ln G(\alpha) &= \ln\left(\frac{0.0048\,AEH(x)}{R}\right) - 1.0516\frac{E}{RT} - \ln\beta \\ &= a + b\ln\beta \qquad (2)\end{aligned}$$

where $G(\alpha)$ is the integral mechanism function, T the absolute temperature, A the pre-exponential factor, R the gas constant, E the apparent activation energy, x the E/RT and β the linear heating rate. On substitution of the values of the conversion degrees at the same temperature on several TG curves, the different mechanism functions $G(\alpha)$ [23] and various heating rates into Eq. 2, the linear correlation coefficient r, the slope b and the intercept a at different temperatures were obtained by a linear least squares method with ln $G(\alpha)$ versus ln β. The corresponding function is the probable mechanism function of a solid phase reaction, if the linear correlation coefficient r is the best while the slope b approaches -1.

The calculation of E and A with the iterative method

The plot of ln β versus $1/T$ by the conventional isoconversional method was inaccurate in calculating the activation energy, as it neglects the variation of $H(x)$ with x. However, the iterative calculations based on consideration of change by means of plots of ln (β/H(x)) versus $1/T$ can give the exact value of activation energy, no matter how little or how great the E/RT value of the reaction is.

The iterative method [22] calculated E is as follows:

Step 1: Assign $H(x) = 1$ to estimate the initial value of the activation energy E_1.

Step 2: Calculate $H(x)$ using E_1, then calculate a new value E_2 from $H(x) = \frac{\exp(-x)}{0.0048\exp(-1.0516x)}h(x)$ via the plot of ln (β/H(x)) versus $1/T$.

Step 3: Repeat step 2, replacing E_1 with E_2, and so on,until the absolute difference of $(E_i - E_{i-1})$ is less than a defined small quantity such as 0.1 kJ mol^{-1}. The last value E_i is the exact value of the activation energy of the reaction. If the reaction mechanism is known, the exact pre-exponential factor A can be calculated from the intercept of the plot at the same time.

Nonlinear integral isoconversional method (NL-INT)

The derivation of the minimum condition is given by Vyazovkin and Dollimore [20] The NL-INT method based on the Eq. 3 minimization.

$$\Omega_{\mathrm{II}}(E_\alpha) = \min\left|\sum_{\mathrm{i}=1}^{n}\sum_{\mathrm{j}\neq \mathrm{i}}^{n}\frac{\beta_{\mathrm{j}}\cdot I\left(E_\alpha, T_{\alpha,\mathrm{i}}\right)}{\beta_{\mathrm{i}}\cdot I\left(E_\alpha, T_{\alpha,\mathrm{j}}\right)} - n(n-1)\right| \qquad (3)$$

By substituting experimental values of T_α and β into Eq. 3 and varying E_α to reach the minimum give the value of the activation energy at a given degree of conversion.

The Starink method [21]

The equation is as follow:

$$\ln\frac{\beta}{T_f^{1.92}} = -1.0008\frac{E}{RT_f} + C \qquad (4)$$

By substituting T_f, β obtained from the experiment into Eq. 4, E is determined from the slope of plots of $\ln(\beta/T_f^{1.92})$ versus $1/T_\mathrm{f}$.

Results and discussion

Elemental analysis

The contents of C, H, N and Ln of the two complexes are shown in Table 1. The experimental data are in good accord with the theoretical values,which indicated that the composition of the complexes conforms to empirical formula of $[\mathrm{Ln(CA)_3bipy}]_2$.

Molar conductance

The title complexes were dissolved in DMSO solution with DMSO as a reference and their molar conductivity were determined ($[\mathrm{Tb(CA)_3bipy}]_2$: 15.5 s cm^2 mol^{-1}; $[\mathrm{Dy(CA)_3bipy}]_2$: 12.2 s cm^2 mol^{-1}).The results show that they are both not electrolyte. The two complexes are stable at room temperature in air. And they are insoluble in water, ethanol and acetone solution and soluble in DMSO and DMF solution.

Infrared spectra

Frequencies of characteristic absorption bands in IR spectra (cm^{-1}) for the ligands and complexes are shown in Table 2. The shift of $\nu_{\mathrm{C=N}}$ (1,578 cm^{-1}) and $\delta_{\mathrm{C-H}}$ (992, 757 cm^{-1}) of bipy ligand to higher strong absorption bands of the two complexes, respectively, can be ascribe to the blockage of respiration vibration and raising energy caused by the two nitrogen atoms coordinated to metal ion, indicating the coordination of the nitrogen atoms of the bipy ligand to the Ln^{3+} ion [24]. The presence of the $\nu_{\mathrm{(Ln-O)}}$ absorption bands, and the appearance of $\nu_{\mathrm{as(COO-)}}$ and $\nu_{\mathrm{s(COO-)}}$ absorption bands of the two complexes and the disappearance of $\nu_{\mathrm{C=O}}$ absorption bands for the acid ligand may suggest the coordination of the oxygen atoms in carboxylic groups to Ln^{3+} ion [25]. Furthermore, $\Delta\nu(\nu_{\mathrm{as}} - \nu_{\mathrm{s}})$ of the two complexes in the range of 221–222 cm^{-1} is higher than that for sodium cinnamate [18] ($\Delta\nu$ = 137 cm^{-1}). This confirms that the carboxy oxygen atoms are probably coordinated to Ln^{3+} ion via unidentate mode[26].

Ultraviolet spectra

The UV spectra data of the ligands and the two complexes were depicted with DMSO solution as reference. The two complexes and ligands have the strong $\pi \rightarrow \pi^*$ transition absorption. The UV absorption spectra of the two complexes show maximum absorption peak at 278 nm, while the band for the HCA ligand is about 270 nm. This phenomenon can be explained by the expansion of π-conjugated system that caused by the metal coordination [27].

Table 2 IR absorption data of the ligands and complexes (cm^{-1})

Ligands and complexes	$\nu_{\mathrm{C=N}}$	$\delta_{\mathrm{C-H}}$	$\nu_{\mathrm{C=O}}$	$\nu_{\mathrm{as(COO-)}}$	$\nu_{\mathrm{s(COO-)}}$	$\nu_{\mathrm{RE\text{-}O}}$
Bipy	1,578	992,757	–	–	–	–
HCA	–	–	1,684	–	–	–
$[\mathrm{Tb(CA)_3bipy}]_2$	1,590	1013,762	–	1,640	1419	417
$[\mathrm{Dy(CA)_3bipy}]_2$	1,585	1013,762	–	1,641	1,419	418

Table 1 Data of elementary analysis of the two title complexes

Complexes	C/%		H/%		N/%		Ln/%	
	Calcd	Found	Calcd	Found	Calcd	Found	Calcd	Found
$[\mathrm{Tb(CA)_3bipy}]_2$	58.74	58.04	3.86	3.33	3.70	3.66	21.01	20.58
$[\mathrm{Dy(CA)_3bipy}]_2$	58.46	58.40	3.85	3.37	3.69	3.58	21.38	21.39

In addition, the maximum absorption band of bipy at 280 nm is similar to that in the two complexes, but it is noteworthy that the molar extinctions coefficient at the same wavelength are greatly enhanced (from 0.28 to 1.70 for $[Tb(CA)_3bipy]_2$; from 0.28 to 1.50 for $[Dy(CA)_3bipy]_2$), suggesting that the two complexes have formed a bigger conjugated system, namely forming a chelating ring.

Thermal decomposition processes

The TG-DTG curves of $[Tb(CA)_3bipy]_2$ (I) and $[Dy(CA)_3 bipy]_2$ (II) at a heating rate of 3 K min^{-1} are shown in Figs. 1 and 2, respectively.

As seen from DTG curves, the thermal decomposition processes for the two complexes can be divided into three stages, respectively. The first stage begins at 369.35 K and terminated at 502.66 K with the mass loss 20.62% (the theoretical loss is 20.64%) in coincidence with the loss of 2bipy for the complex I. The IR spectra of the residue at 502.66 K for the complex I shows the disappearance of absorption band of C=N at 1,590 cm^{-1}. The first stage starts in the range of 384.87–488.94 K with the mass loss of 20.77% which corresponds to the loss of 2 bipy with the theoretical mass loss of 20.55% for the complex II. The IR spectra of the residue at 488.94 K for the complex II shows the disappearance of absorption band of C=N at 1,585 cm^{-1}. Meanwhile, the second and the third step start from 502.66 K to 1,026.84 K with the weight loss of 54.66% (the theoretical loss is 54.65%) which corresponds to the loss of acid ligands for the complex I. The second and the third step start from 488.94 K to 957.24 K with the weight loss 54.67% (the theoretical loss is 54.92%) for the complexII, corresponding to the release acid ligands. The fact indicates that the two complexes have good thermal stability. Eventually, the two complexes were completely degraded into Tb_4O_7 and Dy_2O_3 respectively. The total weight loss of the thermal decomposition process of the complex I is 75.29% (the theoretical mass loss is 75.29%), and that of the complex II is 75.44% (the theoretical mass loss is 75.47%). The characteristic absorption bands of the residue of the two complexes are the same to the standard sample spectra of Tb_4O_7 and Dy_2O_3 as shown in the IR spectra. Based on the analysis above, the thermal decomposition processes of the two complexes can be expressed in the following ways:

$$[Tb(CA)_3bipy]_2 \rightarrow [Tb(CA)_3]_2 \rightarrow Tb_4O_7$$

$$[Dy(CA)_3bipy]_2 \rightarrow [Dy(CA)_3]_2 \rightarrow Dy_2O_3$$

Thermal decomposition kinetics

The activation energy E of the first decomposition stage for the complex $[Tb(CA)_3bipy]_2$ and the complex $[Dy(CA)_3bipy]_2$ have been calculated by the NL-INT methods [20] and the Starink method [21]. Figures 3 and 4 show the relationship between E and α of the first decomposition stage for the two complexes. The value of activation energy E change slightly with α which suggests the

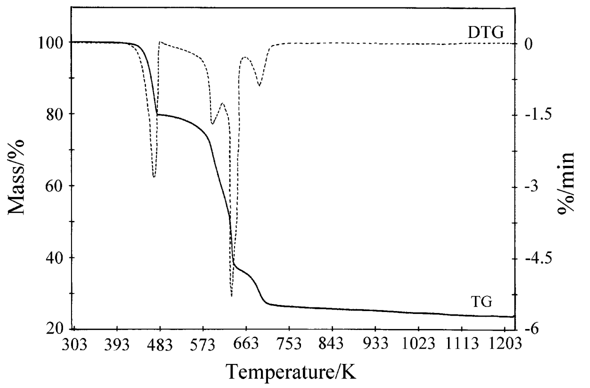

Fig. 1 TG-DTG curves of $[Tb(CA)_3bipy]_2$ ($\beta = 3$ K min^{-1})

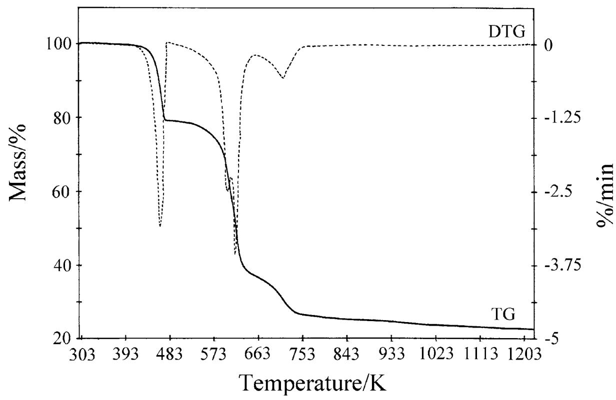

Fig. 2 TG-DTG curves of $[Dy(CA)_3bipy]_2$ ($\beta = 3$ K min^{-1})

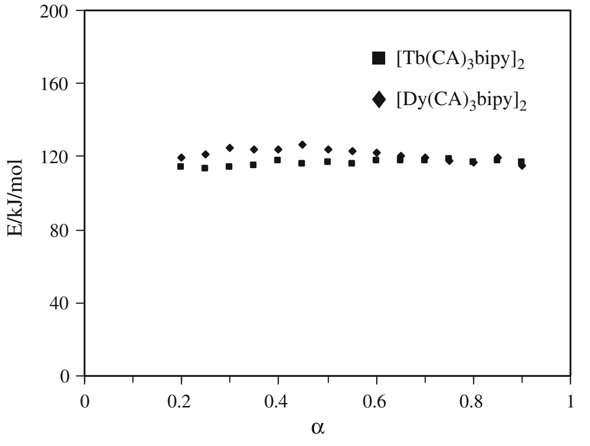

Fig. 3 The relationship of E and α of the first-stage decomposition process with NL-INT method

decomposition stages of the two title complexes are a single step reaction [28]. So the probable mechanism function can be determined by using the double equal-double steps method [19] mentioned above.

The determination of f(α) and G(α)

The values of conversion degrees at the same temperature on five TG-DTG curves of $[Tb(CA)_3bipy]_2$ and $[Dy(CA)_3bipy]_2$ are shown in Tables 3 and 4, respectively By substituting the values of α, β in Tables 3 and 4 and various conversion functions [23] into Eq. 2, the linear correlation coefficient r, the slope b and the intercept a at the different temperatures were obtained by the linear least squares method with $\ln G(\alpha)$ versus $\ln\beta$. The partial results are shown in Tables 5 and 6.

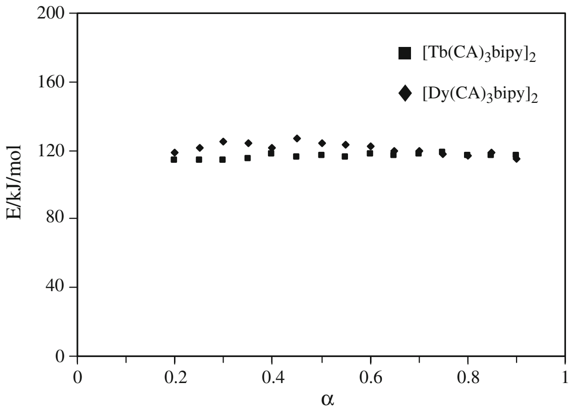

Fig. 4 The relationship of E and α of the first-stage decomposition process with the Starink method

As seen from Table 5, the linear coefficients r of the function No. 14 is the best while the slope b approaches –1 at the five different temperatures. So the probable mechanism function of the first decomposition stage for the complex $[Tb(CA)_3bipy]_2$ is $G(\alpha) = [-\ln(1-\alpha)]^{2/3}$ and $f(\alpha) = 3/2(1-\alpha)[-\ln(1-\alpha)]^{1/3}$. Therefore, the first stage of decomposition is governed by assumed random nucleation and its subsequent growth.

The kinetic equation of this process is $\frac{d\alpha}{dt} = \frac{A}{\beta}\exp\left(-\frac{E}{RT}\right)3/2(1-\alpha)[-\ln(1-\alpha)]^{1/3}$. In the same way, it can

Table 5 Partial results obtained by the linear least squares method at different temperatures for the first stage of $[Tb(CA)_3bipy]_2$

T/K	Function No*	a	b	r
	8	−0.4417	−1.9536	−0.9808
470.52	*14*	0.4988	*−0.9221*	*−0.9823*
	36	0.8187	−0.7043	−0.9265
	8	−0.3678	−1.8780	−0.9792
473.12	*14*	−0.6149	*−0.9759*	*−0.9809*
	36	1.1394	−0.9956	−0.9146
	8	0.3247	−1.8197	−0.9798
474.85	*14*	0.7131	*−1.0295*	*−0.9831*
	36	1.4766	−1.3067	−0.9069
	8	−0.3207	−1.7199	−0.9783
476.49	*14*	0.8176	*−1.0868*	*−0.9826*
	36	0.9634	−1.7616	−0.8968
	8	−0.3585	−1.5843	−0.9723
478.29	*14*	0.8709	*−1.0935*	*−0.9828*
	36	2.3161	−2.0771	−0.9006

The italic values represent the values of the probable mechanism function

* The function No. is from Tables 6–10 in [23]

Table 3 Conversion degrees measured for given the same temperatures on five TG-DTG curves of $[Tb(CA)_3bipy]_2$ at different heating rates for the first stage

T/K	α				
	$\beta = 3\ \mathrm{K\ min^{-1}}$	$\beta = 5\ \mathrm{K\ min^{-1}}$	$\beta = 7\ \mathrm{K\ min^{-1}}$	$\beta = 10\ \mathrm{K\ min^{-1}}$	$\beta = 15\ \mathrm{K\ min^{-1}}$
470.52	0.7276	0.4694	0.2500	0.2374	0.1255
473.12	0.8394	0.5558	0.3000	0.2870	0.1512
474.85	0.9079	0.6233	0.3500	0.3248	0.1701
476.49	0.9590	0.6995	0.4000	0.3650	0.1963
478.29	0.9764	0.7675	0.4500	0.4132	0.2249

Table 4 Conversion degrees measured for given the same temperatures on five TG-DTG curves of the $[Dy(CA)_3bipy]_2$ at different heating rates for the first stage

T/K	α				
	$\beta = 3\ \mathrm{K\ min^{-1}}$	$\beta = 5\ \mathrm{K\ min^{-1}}$	$\beta = 7\ \mathrm{K\ min^{-1}}$	$\beta = 10\ \mathrm{K\ min^{-1}}$	$\beta = 15\ \mathrm{K\ min^{-1}}$
467.67	0.7421	0.3523	0.2500	0.1479	0.1327
469.78	0.8490	0.4198	0.3000	0.1804	0.1584
471.39	0.9175	0.4804	0.3500	0.2111	0.1808
473.11	0.9679	0.5465	0.4000	0.2456	0.2075
474.23	0.9803	0.5930	0.4500	0.2724	0.2293

Table 6 Partial results obtained by the linear least squares method at different temperatures for the second stage of [Dy(CA)$_3$bipy]$_2$

T/K	Function No*	a	b	r
467.67	16	0.7114	−1.4225	−0.9683
	25	*0.3513*	*−1.1075*	*−0.9803*
	33	0.3712	−0.8694	-0.9858
469.78	16	0.8875	−1.5125	−0.9684
	25	*0.4104*	*−1.0904*	*−0.9856*
	33	0.3748	−0.8059	−0.9898
471.39	16	1.0241	−1.5721	−0.9654
	25	*0.4300*	*−1.0436*	*−0.9874*
	33	0.3552	−0.7291	−0.9882
473.11	16	1.1899	−1.6654	−0.9616
	25	*0.4399*	*−0.9928*	*−0.9902*
	33	0.3323	−0.6554	−0.9854
474.23	16	1.2563	−1.6770	−0.9634
	25	*0.4332*	*−0.9406*	*−0.9910*
	33	0.3129	−0.6000	−0.9790

The italic values represent the values of the probable mechanism function

* The function No. is from Tables 6–10 in [23]

be easily seen from Table 6 that the function No. 25 is the probable mechanism function of the first decomposition stage for the complex [Dy(CA)$_3$bipy]$_2$, i.e., $G(\alpha) = \alpha$ and $f(\alpha) = 1$. Therefore, it can be decided that the reaction mechanism in the first stage of the complex [Dy(CA)$_3$bipy]$_2$ is the boundary reaction. The kinetic equation of this process is $\frac{d\alpha}{dt} = \frac{A}{\beta}\exp\left(-\frac{E}{RT}\right)$.

The calculation of E and A

The values of temperature for the first thermal decomposition at the same degree of conversion on five curves of the complex [Tb(CA)$_3$bipy]$_2$ is listed in Table 7 and those of [Dy(CA)$_3$bipy]$_2$ is listed in Table 8. By substituting the values of α, β and T in Tables 7 and 8 and the corresponding mechanism function determined above into Eq. 1, via the linear least squares method with $ln\beta/H(x)$ versus $1/T$, the activation energy E can be calculated from the value of the slope, and the pre-exponential factor A can also be calculated from the value of the intercept. The results above are listed in Tables 7 and 8, respectively.

The thermodynamic parameters of activation can be calculated from the equations [29, 30].

$$A\exp(-E/RT) = v\exp\left(\Delta G^{\neq}/RT\right) \tag{5}$$

$$\Delta H^{\neq} = E - RT \tag{6}$$

$$\Delta G^{\neq} = \Delta H^{\neq} - T\Delta S^{\neq} \tag{7}$$

where v is the Einstein Vibration frequency, $v = k_B\ T/h$ (where k_B and h are Boltzmann and Planck constants, respectively), $\Delta G^{\neq}$ the Gibbs free energy of activation, $\Delta H^{\neq}$ the enthalpy of activation, $\Delta S^{\neq}$ entropy of activation. The values of entropy, enthalpy and the Gibbs free energy of activation at the peak temperature obtained on the basis of Eqs. 5–7 are shown in Tables 9 and 10.

From Tables 9 and 10, it can be clearly seen that the values of $\Delta G^{\neq} > 0$ for the two complexes indicate that their decomposition reaction are not spontaneous reactions.

Table 7 Temperatures corresponding to the same degree of conversion at different heating rates for [Tb(CA)$_3$bipy]$_2$ (Stage I)

α	T/K						
	3 K min^{-1}	5 K min^{-1}	7 K min^{-1}	10 K min^{-1}	15 K min^{-1}	E/kJ mol^{-1}	$A \times 10^{11}$/min^{-1}
0.20	453.13	459.44	467.46	467.93	476.70	119.55	24.23
0.25	455.94	462.31	470.52	471.14	479.93	122.16	50.42
0.30	458.39	464.65	473.12	474.09	482.24	125.29	118.76
0.35	460.24	466.94	474.85	475.81	484.39	124.85	108.23
0.40	462.25	468.49	576.49	478.03	485.97	124.70	106.92
0.45	463.50	470.07	478.29	479.78	487.70	127.29	213.11
0.50	465.13	471.53	479.78	481.01	489.37	124.52	104.67
0.55	466.31	472.78	481.00	482.65	490.74	123.40	79.17
0.60	467.96	473.98	482.19	483.80	492.09	122.93	69.58
0.65	468.67	475.38	483.31	485.38	493.16	120.50	36.99
0.70	470.05	476.52	484.27	486.52	494.72	120.09	33.04
0.75	471.15	477.72	485.39	487.65	495.77	117.99	19.07
0.80	471.97	478.84	486.52	488.87	497.08	117.43	16.22
0.85	473.23	480.00	487.66	490.39	498.40	119.64	28.58
0.90	474.45	481.44	488.85	491.83	499.77	115.61	9.71

Table 8 Temperatures corresponding to the same degree of conversion at different heating rates for $[Dy(CA)_3bipy]_2$ (Stage I)

α	T/K						
	3 K min^{-1}	5 K min^{-1}	7 K min^{-1}	10 K min^{-1}	$\beta = 15$ K min^{-1}	E/kJ mol^{-1}	$A \times 10^{11}/min^{-1}$
0.20	451.46	461.15	465.38	470.84	472.74	119.55	24.23
0.25	454.17	463.82	467.67	473.55	475.08	122.16	50.42
0.30	456.48	465.76	469.78	475.44	477.24	125.29	118.76
0.35	458.24	467.61	471.39	477.41	479.28	124.85	108.23
0.40	459.56	469.06	473.11	478.73	480.86	124.70	106.92
0.45	461.28	470.61	474.23	480.39	482.15	127.29	213.11
0.50	462.41	471.74	475.49	482.02	483.82	124.52	104.67
0.55	463.43	473.18	476.34	483.25	485.30	123.40	79.17
0.60	464.63	474.27	478.15	484.65	486.57	122.93	69.58
0.65	465.62	475.58	479.16	486.07	488.22	120.50	36.99
0.70	466.79	476.54	480.37	487.28	489.67	120.09	33.04
0.75	467.78	471.63	481.43	488.88	490.93	117.99	19.07
0.80	468.94	478.90	482.67	490.01	492.61	117.43	16.22
0.85	469.93	479.99	483.73	490.17	493.87	119.64	28.58
0.90	471.14	481.51	485.41	492.76	475.41	115.61	9.71

Table 9 The thermodynamic parameters for $[Tb(CA)_3bipy]_2$ (Stage I)

β/ K min^{-1}	$\Delta G^{\neq}$/ kJ mol^{-1}	$\Delta H^{\neq}$/ kJ mol^{-1}	$\Delta S^{\neq}$/ J mol^{-1} K^{-1}	Tp/K
3	122.87	113.03	−20.91	470.85
5	123.04	112.96	−21.05	478.82
7	123.16	112.91	−21.15	484.55
10	123.22	112.89	−21.20	487.48
15	123.40	112.81	−21.34	496.16

Table 10 The thermodynamic parameters for $[Dy(CA)_3bipy]_2$ (Stage I)

β/ K min^{-1}	$\Delta G^{\neq}$/ kJ mol^{-1}	$\Delta H^{\neq}$/ kJ mol^{-1}	$\Delta S^{\neq}$/ J mol^{-1} K^{-1}	Tp/K
3	123.09	117.87	−11.28	467.26
5	123.20	117.73	−11.46	477.37
7	123.23	117.71	−11.51	480.22
10	123.34	117.63	−11.66	488.93
15	123.35	117.62	−11.68	490.38

Conclusions

The two lanthanide complexes of $[Tb(CA)_3bipy]_2$ and $[Dy(CA)_3bipy]_2$ were synthesized and characterized. Their mechanism functions of the first-stage thermal decomposition procedure were determined. Meanwhile, the enthalpy of activation $\Delta H^{\neq}$, the Gibbs free energy of activation $\Delta G^{\neq}$, the entropy of activation $\Delta S^{\neq}$ at the peak temperature, the activation energy E and the pre-exponential factor A were obtained, respectively.

Acknowledgements This project was supported by the National Natural Science Foundation of China (No. 20773034), the Natural Science Foundation of Hebei Province (No. B2007000237, No. E2009000307) and Education Department Scientific Research Fund from Hebei Province (2008469).

References

1. Yan B. Sol–gel preparation and luminescence of silica/polymer hybrid material incorporated with terbium complex. Mater Lett. 2003;57:2535–9.
2. Ci YX, Li YZ, Chang WB. Fluorescence reaction of terbium(III) with nucleic acids in the presence of phenanthroline. Anal Chim Acta. 1991;248:589–94.
3. Scott LK, Horrocks WD. Lanthanide ion luminescence as a probe of DNA structure. 2. Non-guanine-containing oligomers and nucleotides. J Inorg Biochem. 1992;46:193–205.
4. Siqueira AB, Bannach G, Rodrigues EC, Carvalho CT, Ionashiro M. Solid-state 2-methoxybenzoates of light trivalent lanthanides synthesis, characterization and thermal behaviour. J Therm Anal Cal. 2008;91:897–902.
5. Locatelli JR, Rodrigues EC, Siqueira AB, Ionashiro EY, Bannach G, Ionashiro M. Synthesis characterization and thermal behaviour of solid-state compounds of yttrium and lanthanide benzoates. J Therm Anal Cal. 2007;90:737–46.
6. Li Y, Zheng FK, Liu X, Zou WQ, Guo GC, Lu CZ, et al. Crystal structures and magnetic and luminescent properties of a series of homodinuclear lanthanide complexes with 4-cyanobenzoic ligand crystal structures and magnetic and luminescent properties of a series of homodinuclear lanthanide complexes with 4-cyanobenzoic ligand. Inorg Chem. 2006;45:6308–16.
7. Li GQ, Li Y, Zou WQ, Chen QY, Zheng FK, Guo GC. Synthesis and crystal structure of a new Lanthanum(III) 4-cyanobenzoate complex. Chin J Struct Chem. 2007;26:575–9.
8. Lam AWH, Wang W, Gao TS, Wen GH, Zhang XX. Synthesis, crystal structure, and photophysical and magnetic properties of dimeric and polymeric lanthanide complexes with benzoic acid and its derivatives. Eur J Inorg Chem 2003;2003:149–63.

9. Ferenc W, Dziewulska-Kuaczkowska A, Sarzyski J, Paszkowska B. 4-Chloro-2-methoxybenzoates of heavy lanthanides(III) and yttrium(III) Thermal spectral and magnetic behaviour. J Therm Anal Cal. 2008;91:285–92.
10. Ionashiro EY, Bannach G, Siqueira AB, de Carvalho CT, Rodrigues EC, Ionashiro M. 2-Methoxybenzylidenepyruvatewith heavier trivalent lanthanides and yttrium(III) synthesis and characterization. J Therm Anal Cal. 2008;92:953–9.
11. Tian L, Ning Ren, Zhang JJ, Sun SJ, Ye HM, Bai JH, et al. Synthesis, crystal structure, and thermal decomposition kinetics of the complex of dysprosium benzoate with 2, 2′-bipyridine. J Chem Eng Data. 2009;54:69–74.
12. Xu XL, Zhang JJ, Yang HF, Ren N, Zhang HY. Synthesis, crystal structure and thermal decomposition of a dysprosium(III) p-fluorobenzoate 1, 10-phenanthroline complex. J Chem Sci. 2007;62b: 51–4.
13. Zhang HY, Zhang JJ, Ren N, Xu SL, Tian L, Bai JH. Synthesis, crystal structure and thermal decomposition mechanism of the complex $[Sm(p\text{-BrBA})_3bipy \cdot H_2O]_2 \cdot H_2O$. J Alloy Compd. 2008;464: 277–81.
14. Zhang JJ, Ren N, Bai JH, Xu SL. Synthesis and thermal decomposition reaction kinetics of complexes of $[Sm_2(m\text{-ClBA})_6(phen)_2] \cdot 2H_2O$ and $[Sm_2(m\text{-BrBA})_6(phen)_2] \cdot 2H_2O$. J Chem Kinet. 2007;39:67–74.
15. Tian L, Ren N, Zhang JJ, Liu HM, Bai JH, Ye HM, et al. Synthesis, crystal structure luminescence and thermal decomposition kinetics of Eu(III) complex with 2, 4-dichlorobenzoic acid and 2, 2′-bipyridine. Inorg Chim Acta. 2009;362:3388–94.
16. Guo DF, He J, Zeng ZZ. Studies on interaction between ternary rare earth complexes of cinnamic acid and phenanthroline with DNA by spectroscopy. J Chin Rare Earth Soc. 2004;22:55–60.
17. Carvalho Filho MAS, Fernandes NS, Leles MIG, Mendes R, Ionashiro M. Preparation and thermal decomposition of solid-state cinnamates of lighter trivalent lanthanides. J Therm Anal Cal. 2000;59:669–74.
18. Xie XM, Zeng ZZ. Syntheses, anti-inflammatory action and XPS of Ln (III) -1, 10-phenanthroline-cinnamic acid complexes. J Lanzhou Univ (Nat Sci). 2003;39:64–7.
19. Zhang JJ, Ren N. A new kinetic method of processing TA data. Chin J Chem. 2004;22:1459–62.
20. Vyazovkin S, Dollimore D. Linear and nonlinear procedures in isoconversional computations of the activation energy of non-isothermal reactions in solids. J Chem Inf Comp Sci. 1996;36: 42–5.
21. Starink MJ. The determination of activation energy from linear heating rate experiments: a comparison of the accuracy of iso-conversion methods. Thermochim Acta. 2003;404:163–76.
22. Gao Z, Nakada M, Amasski I. A consideration of errors and accuracy in the isoconversional methods. Thermochim Acta. 2001;369:137–42.
23. Hu RZ, Gao SL, Zhao FQ, Shi QZ, Zhang TL, Zhang JJ. Thermal Analysis Kinetics. 2nd ed. Beijing: Science Press; 2008. p. 151.
24. Wang RF, Jin LP, Wang MZ, Huang SH, Chen XT. Synthesis, crystal structure and luminescence of coordination compound of europium p-methylbenzoate with 2, 2′-Dipyridine. Acta Chim Sin. 1995;53:39–45.
25. Shi YZ, Sun XZ, Jiang YH. Spectra and Chemical Identification of Organic Compounds. Nanjing: Science and Technology Press; 1988. p. 98.
26. Deacon GB, Phillips RJ. Relationships between the carbon-oxygen stretching frequencies of carboxylato complexes and the type of carboxylate coordination. Coord Chem Rev. 1980;33:227–50.
27. An BL, Gong ML, Li MX, Zhang JM. Synthesis, structure and luminescence properties of samarium(III) and dysprosium(III) complexes with a new tridentate organic ligand. J Mol Struct. 2004;687:1–6.
28. Lu ZR, Ding YC, Xu Y, Li BL, Zhang Y. TA Study on four-one-dimensional chain copper complexes with benzoylacetone or 1, 1, 1-trifluoro-3-(2-thenoyl)-acetone bridged through azobispyridine ligands. Chin J Inorg Chem (in Chinese). 2005;21:181–5.
29. Straszko J, Olstak-Humienik M, Mozejko J. Kinetics of thermal decomposition of $ZnSO_4 \cdot 7H_2O$. Thermochim Acta. 1997;292: 145–50.
30. Olstak-Humienik M, Mozejko J. Thermodynamic functions of activated complexes created in thermal decomposition processes of sulphates. Thermochim Acta. 2000;344:73–9.